Science of the Total Environment 775 (2021) 145689

Contents lists available at ScienceDirect

Science of the Total Environment

journal homepage: www.elsevier.com/locate/scitotenv

Long-term and multilevel impact assessment of the 2015–2016 El Niño on a sandy beach of the southwestern Atlantic

Gabriela Jorge-Romero [a,*], Eleonora Celentano [a], Diego Lercari [a], Leonardo Ortega [b], Juan A. Licandro [a], Omar Defeo [a]

[a] Universidad de la República, Facultad de Ciencias, Departamento de Ecología y Evolución, UNDECIMAR, Iguá 4225, PO Box 10773, Montevideo 11400, Uruguay
[b] Dirección Nacional de Recursos Acuáticos, Constituyente 1497, Montevideo 11200, Uruguay

HIGHLIGHTS

- El Niño disrupted a sandy beach system at all levels of ecological organization
- Drastic increases in sea temperature, rainfall and freshwater runoff were quantified
- The structural and functional restructuring prompted a loss of ecosystem resilience
- The system showed hysteresis and was unable to recover after two years of the event
- A transitional community state dominated by polychaetes was set after El Niño

GRAPHICAL ABSTRACT

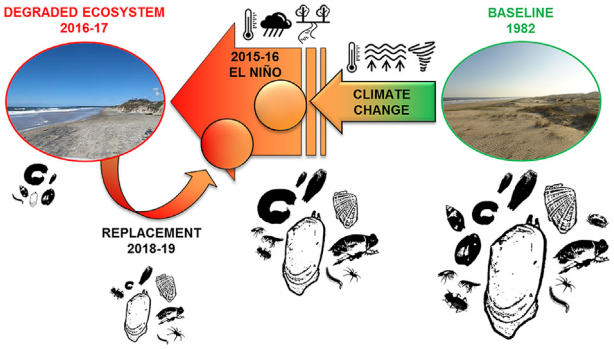

ARTICLE INFO

Article history:
Received 10 December 2020
Received in revised form 21 January 2021
Accepted 3 February 2021
Available online 15 February 2021

Editor: Martin Drews

Keywords:
El Niño Southern Oscillation
Press and pulse perturbations
Sandy shores
Ecosystems
Trophic models
Uruguay

ABSTRACT

As a land-sea interface, the fingerprints of climate perturbations may be immediately and profoundly felt in sandy beaches and the macroinvertebrates they harbour. In particular, extreme climatological events can result in long-lasting or irreversible ecological changes, and therefore, it has become critical to understand how these ecosystems respond to strong pulse perturbations. This study assessed the main impacts prompted by the 2015–2016 El Niño on a Southwestern Atlantic sandy beach ecosystem. A long-term (1982–2019) analysis was carried out, attending historical climate components and multilevel indicators of change across levels of ecological organization. The trophic networks of four ecosystem states were compared, and the macroinvertebrate community structure was analysed in terms of species richness, abundance and biomass and deconstructed by taxonomy, beach zone occupied, feeding, and development modes. The potential recovery pathway of the system was also assessed. Climatic effects were reflected in a marked increase in sea surface temperature anomalies, rainfall, and in the discharge of the widest estuary of the world (Río de la Plata). An abrupt disruption of ecological attributes due to El Niño effects was evidenced. After the event, the ecosystem shifted to a higher organization of the flow structure (Ascendency), a lower adaptive potential (Overhead), and a marked increase in efficiency (Robustness), reflecting a more vulnerable state to absorb disturbances. The decrease in species abundance and biomass was particularly noticeable in molluscs, filter feeders, and low intertidal/subtidal groups. By

Abbreviations: BCB, Barra del Chuy Beach; CC, Climate change; ENSO, El Niño-Southern Oscillation; PP, Primary production; RdlP, Río de la Plata; SST, Sea surface temperature; SSTA, Sea surface temperature anomalies; SAO, Southwestern Atlantic Ocean.

* Corresponding author.
E-mail address: gabriela.t.jorge@gmail.com (G. Jorge-Romero).

https://doi.org/10.1016/j.scitotenv.2021.145689

contrast, polychaetes/deposit feeders were favoured, triggering a transitional community state dominated by opportunistic species. The results highlight how extreme climatic events could prevent the recovery of a sandy beach ecosystem, as pulses may induce lag and legacy effects.

1. Introduction

Perceived as ecosystems at risk, sandy beaches are under great pressure and are increasingly affected by a variety of anthropogenic and natural hazards acting simultaneously at multiple temporal and spatial scales (Defeo et al., 2009; McLachlan and Defeo, 2018; Fanini et al., 2020). As a land-sea interface, the fingerprints of climate change (CC) may be immediately and profoundly felt in sandy beaches and the macroinvertebrates they harbour, a consequence of increasing erosion coupled with sea-level rise, storminess, and onshore winds (Schoeman et al., 2014; Bindoff et al., 2019). When combined with the long-term stress imposed by CC, extreme climatological events (the 'press and pulse' framework; Smith, 2011) can result in long-lasting or irreversible ecological changes (Harris et al., 2020). Thus, it has also become critical to understand how these ecosystems respond to strong pulse perturbations (McLachlan et al., 2013; McLachlan and Defeo, 2018; Cavanaugh et al., 2019).

The El Niño-Southern Oscillation (ENSO) is the dominant mode of interannual climate variability across the Pacific Ocean basin, severely disrupting global climate patterns (Wolter, 1987; Barnard et al., 2017; Cai et al., 2020). ENSO exhibits two opposite phases defined by an anomalous cooling (La Niña) and a warming (El Niño) phase, causing large-scale changes in ocean and atmospheric circulation and increasing the likelihood of extreme climatic events (including storms, floods, and droughts) with strong repercussions on human well-being (Santoso et al., 2017). As a pseudocyclical phenomenon, ENSO occurs irregularly every two to seven years, making its prediction difficult. As CC unfolds, El Niño events develop in a warmer mean state, leading to thermal stress (Bertrand et al., 2020). Thus, climate model projections suggest an increase in the frequency and intensity of El Niño extreme events (Cai et al., 2014; Santoso et al., 2017), potentially triggering profound social-ecological consequences on coastal ecosystems, including sandy beaches (McLachlan and Defeo, 2018). Marked El Niño effects in sandy shores have been evidenced both on the physical environment (Barnard et al., 2017; Orlando et al., 2019) and at different levels of ecological organization, including ecosystems (Revell et al., 2011), communities (Arntz et al., 1987), and populations (Riascos et al., 2009; Ortega et al., 2012).

Ocean warming displays a clear signal in the Southwestern Atlantic Ocean (SAO), particularly over the continental shelf of southern Brazil, Uruguay, and northern Argentina, which comprise one of the largest and most energetic marine hotspots worldwide (Hobday and Pecl, 2014). The adjacent Río de la Plata (RdlP) basin is also subject to intense warming (Franco et al., 2020). Sea surface temperature anomalies (SSTA) have shown an increasing trend over time, particularly after shifting from a cold to a warm period during the 1990s (Ortega et al., 2016). The position of the warm waterfront of the Brazil Current evidenced a consistent long-term poleward shift (Gianelli et al., 2019a), and the advection of warm waters into the northeast Uruguayan slope has been enhanced by the increase in speed and frequency of onshore winds (Ortega et al., 2013). Ocean warming has been responsible for the occurrence of mass mortality events in species with a cool-water affinity (Ortega et al., 2016), the increasing occurrence of harmful algal blooms (Martínez et al., 2017; Gianelli et al., 2019b) and a shift from cool-water to warm-water species in the relative representation of Uruguayan fisheries landings (Gianelli et al., 2019a). The RdlP Estuary drains the fourth largest river basin in the world and the second largest of South America. Its plume enters the Southwestern Atlantic continental shelf and spreads along the coasts of Argentina, Uruguay, and Brazil (Piola et al., 2005). The interannual variability of the RdlP discharge is closely associated with ENSO cycles, which partially modulate the plume dynamics (Piola et al., 2005). Large precipitation anomalies over the RdlP basin associated with El Niño events significantly increase the river discharge (Piola et al., 2005; Bodnariuk et al., 2021), producing a significant decrease in salinity along the Uruguayan shelf (Ortega and Martínez, 2007). The intensity of the signal is seasonally dependent, with the greatest impact registered from spring to the end of summer (Pisciottano et al., 1994; Cazes-Boezio et al., 2003). In particular, the 2015–2016 El Niño was recognized as one of the three strongest events in the past 145 years, similar to 1982–1983 and 1997–1998 (Herring et al., 2018; Wang et al., 2019; https://ggweather.com/enso/oni.htm, last accessed November 2020). By October 2014, the above average sea surface temperature (SST) in the El Niño 3.4 region indicated the development of the event, which persisted throughout 2015 and dissipated during late May/early June 2016 (https://origin.cpc.ncep.noaa.gov/products/analysis_monitoring/ensostuff/ONI_v5.php, last accessed November 2020). The 2015–2016 El Niño prompted a sharp increase in rainfall and in the freshwater discharge of the RdlP in April 2016, hitting the Atlantic coast of Uruguay as a strong pulse perturbation.

The dissipative Barra del Chuy beach (BCB), located on the Atlantic coast of Uruguay, shows high autochthonous primary production (PP) and supports rich benthic macrofauna that have sustained a small-scale fishery since the last century (Lercari et al., 2018). At BCB, long-term scientific evidence shows tropicalization of the filter-feeding guild, which includes a decline in abundance of the cold-water yellow clam *Mesodesma mactroides* and an increase in the relative representation of the mole crab *Emerita brasiliensis*, a species with tropical affinities (Celentano and Defeo, 2016). These changes have been mainly attributed to a systematic increase in SST- and related CC-driven stressors (Ortega et al., 2016). Food web-based ecosystem indicators (Ulanowicz, 1986, 2004, 2014) have reflected a low resilience of BCB and therefore a highly vulnerable system to face unexpected disturbances such as those imposed by the 2015–2016 El Niño, which could have disrupted internal ecosystem cycling.

This study assessed the effects of the 2015–2016 El Niño on the structure and functioning of the BCB ecosystem. A multilevel analysis was carried out through a long-term (1982–2019) before-after framework, attending changes at different levels of ecological organization, including the ecosystem trophic network and the macroinvertebrate community. The latter was deconstructed to discriminate among taxonomic groups, supralittoral and intertidal forms, and groups with different feeding habits and development modes. The potential recovery pathway of the system was also assessed.

2. Materials and methods

2.1. Study area

The study was performed at BCB (33°40′S; 53°20′W) located on the eastern coast of Uruguay in the SAO (Fig. 1). This dissipative beach is characterized by fine to very fine well-sorted sands (mean grain size = 0.20 mm, sorting = 0.70 mm), a gentle beach slope (slope = 3.53%), and a wide surf zone (Lercari et al., 2010). The high productivity of this microtidal system (tidal range = 0.5 m) supports the greatest macrofaunal richness, diversity, abundance and biomass among Uruguayan beaches (Lercari and Defeo, 2006, 2015). The BCB is delimited by two freshwater discharges, a natural discharge in the NE (Chuy Stream) and an artificial discharge in the SW (Andreoni Canal). Both discharges

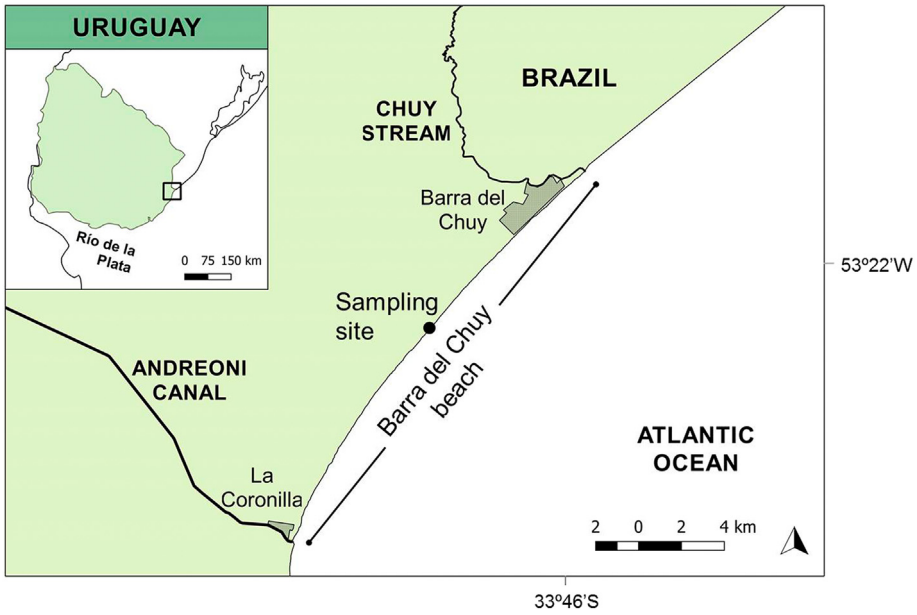

Fig. 1. Study area, showing the location of Barra del Chuy beach along the eastern coast of Uruguay in the Southwestern Atlantic Ocean.

generally follow a SW–NE direction. The Canal drains a wide basin used for agricultural activities, affecting the beach quality around La Coronilla town (Lercari et al., 2002; Jorge-Romero et al., 2019) with 1153 residents (https://www.ine.gub.uy/web/guest/343, last accessed January 2021). On the NE extreme of the beach, Barra del Chuy town has only 370 inhabitants (https://www.ine.gub.uy/web/guest/343, last accessed January 2021). The selected sampling site, located 13 km away from the mouth of the Canal (Fig. 1), is considered undisturbed by urbanization and the effects of both freshwater discharges (Lercari et al., 2002; Jorge-Romero et al., 2019).

2.2. Tracking the signal

2.2.1. Data source

SSTA and satellite precipitation data were obtained from the IRI/LDEO Climate Data Library datasets of the National Climatic Data Center (https://iridl.ldeo.columbia.edu/, last accessed November 2020; Grumbine, 1996; May et al., 1998; Cavalieri et al., 1997; Reynolds et al., 2007; and Janowiak et al., 1999, respectively). To describe long-term trends of ocean climate, SSTA was calculated by averaging 8° × 9° grid cells (30°S-39°S; 60°W-52°W) of the SAO shelf and the adjacent oceanic region. The SSTA was also linearly detrended to reflect the actual variability in the SSTA patterns rather than long-term trends towards warming in the area. Likewise, precipitation in the RdlP basin region was calculated by averaging 18° × 11° grid cells (25°S-36°S; 70°W-52°W) and standardized by computing the difference between monthly climatology (long-term mean 1979–1995) and the original data, and dividing the resulting estimate by the standard deviation using IRI expert mode functions facilities. Monthly RdlP discharge (Q, $m^3.s^{-1}$) was obtained from Instituto Nacional del Agua, Argentina (https://www.ina.gov.ar/, last accessed November 2020); the Q anomaly was calculated by computing the difference between long-term monthly climatology estimates (1982–2018) and the original data. SSTA, rainfall, and Q were averaged between September and April, when ENSO had the highest impacts in the RdlP basin (Cazes-Boezio et al., 2003; Robertson and Mechoso, 1998, 2003).

Almost 40 years (1982–2019) of intensive field surveys were dumped to disentangle the ecological responses of BCB to the pressures imposed by the 2015–2016 El Niño using a before-after approach. Macrofaunal abundance and biomass estimates were obtained through systematic sampling. Three transects spaced 8 m apart were set perpendicular to the shoreline, with sampling units at 4 m intervals starting at the base of the dunes and continuing in a seaward direction to the lower limit of the swash zone, determined by the minimum tide advance during the sampling period. In each sampling unit, a sheet metal cylinder 16 cm in diameter and 40 cm in depth was used. Each individual retained after sieving through a 0.5 mm mesh was fixed in 5% formalin for later analysis, including species identification, counting, and weight determinations (0.0001 g) (Brazeiro and Defeo, 1996).

Complementary input data for ecosystem modelling comprised values gathered from published and unpublished information for the study area and from empirical relationships (see Supplementary Materials A). Phytoplankton biomass was estimated from in vivo pigment fluorescence (2016 unpublished data; see Cremella et al., 2018 for conversion and correction algorithms) and converted to wet biomass (Odebrecht et al., 1995). Zooplankton biomass was obtained from Lercari et al. (2010). Fish biomass was estimated based on trawl samples parallel to the coast (Lercari et al., 2018). Bird biomass was estimated based on richness and abundance surveys (Lercari et al., 2018). Detritus biomass was estimated in situ from total suspended solids, considering fractions of living (phytoplankton) and inorganic materials (Lercari et al., 2010).

2.2.2. Ecosystem modelling

The chosen strategy comprised a long-term comparison of four ecosystem states before (n = 2) and after (n = 2) the occurrence of the 2015–2016 El Niño event. A baseline scenario developed by Lercari et al. (2018) for 1982 allows us to grasp long-term changes. Three trophic models were built to capture the state before (2013) and immediately after El Niño (spring 2016 to autumn 2017) and to track changes up to 2018. The four scenarios were modelled through Ecopath with Ecosim 6 (EwE 6), which allows the representation of ecosystems as interconnected networks of trophic groups based on biomass and linked by diet information (Polovina, 1984; Christensen and Pauly, 1992). As a mass-balanced model, each functional group (species with similar life-history traits and ecological role) was represented by a linear equation that describes how group production equals the sum of the entire group losses (Christensen and Pauly, 1998; Christensen and Walters, 2004; Christensen et al., 2005), as follows:

$$B_i(P/B)_i - \sum_{j-1}^{n} B_j(Q/B)_j DC_{ji} - Y_i - B_i(P/B)_i - (1 - EE_i) = 0$$

where B_i and B_j are the biomasses of prey and predators, respectively; $(P/B)_i$ is the production/biomass ratio; $(Q/B)_j$ is the consumption/

biomass ratio for predator j; DC_{ji} is the fraction of prey i in the diet of predator j; Yi is the total fishery catch rate; and EE_i is the ecotrophic efficiency, defined as the proportion of production i that is utilized in the system.

Whenever possible, functional groups were defined at the species level, including detritus, phytoplankton, zooplankton, the macrobenthic community, insects, fishes, and birds. P/B and Q/B ratios were taken from published information or empirical relationships (Brey, 2012) and corrected for local SST (NOAA; https://iridl.ldeo.columbia.edu/, last accessed November 2020). DC estimates were mainly compiled from published information, qualitative records, and general knowledge of the trophic ecology of the groups (see Supplementary Materials B and C for input data and diet information, respectively).

The Pedigree index was calculated (Pauly et al., 2000; Christensen and Walters, 2004), and model quality was classified according to Lassalle et al. (2014). The theoretical and practical rigor of each model was validated through prebalance diagnosis (PREBAL: Link, 2010), ensuring confidence in model design and parameterization (see Supplementary Materials D). Physiological system constraints were assured according to Christensen et al. (2008) and Heymans et al. (2016). Given the general strategy used to attain mass balance, only slight modifications of diet input data were needed.

Several ecosystem attributes based on Ulanowicz theory (1986) were assessed to characterize the system in terms of its structure and functioning (Christensen et al., 2005): (1) The Total System Throughput (TST), ecosystem size in terms of biomass flows, defined as the sum of all flows in the system (consumption, respiration, exports, imports, and detritus). (2) The System Omnivory Index (SOI), the extent to which an ecosystem exhibits web-like features. The SOI strongly correlates with system maturity and stability. (3) Ascendency (A), a measure of the average mutual information (organization of the flow structure) in a system, scaled by TST. It characterizes the degree of development and organization of the system. (4) Capacity (C), the upper limit of the size of A, which represents the maximum potential of ecosystem development. (5) Overhead (O), the difference between C and A, which represents the ecosystem potential for recovery or innovative restructuring to face unexpected perturbations (e.g., resilience). The Robustness index (Ulanowicz, 2014; Fath, 2015) was also quantified to analyse ecosystem sustainability in terms of growth (e.g., total system throughput) and development (e.g., information or connectivity). It measures the probability that a system lies within its upper and lower boundary when exposed to a certain stress factor (Mumby et al., 2014). The compromise between efficiency and resilience was assessed by positioning each model on a hypothetical curve of "ecosystem fitness for evolution" ($-A/C * \ln(A/C)$) vs. "degree of order" ($a = A/C$ ($1 > a > 0$)).

2.2.3. Community structure

A 16-year time-series dataset of the macroinvertebrate (benthos plus insects) community was analysed to assess the structural and functional changes in the 2015–2016 ENSO-associated anomalies (before: 2006–2013, during: autumn 2016, and after: spring 2016 to summer 2019). Community abundance and biomass for the years 2014 and 2015 were estimated based on the interpolation of the previous and following years due to logistical difficulties that prevented the continuity of the surveys. To assess temporal fluctuations in the abundance and biomass of the macroinvertebrate community, non-metric multidimensional scaling (NMDS) analysis was performed with PRIMER-6 software (Anderson et al., 2015) to obtain two-dimensional (2D) ordination of Bray–Curtis distances between pairs of samples from different times based on root–root transformed data. A one-way PERMANOVA (Anderson et al., 2015) was performed to assess differences in community structure, both for abundance and biomass, using root-root transformed data and the Bray–Curtis similarity index for three-year periods before and after El Niño.

2.2.4. Deconstructive approach

Unlike when only aggregate richness is considered, different groups of disaggregated species may exhibit contrasting patterns in response to El Niño effects. Thus, deconstructing biodiversity could provide a more

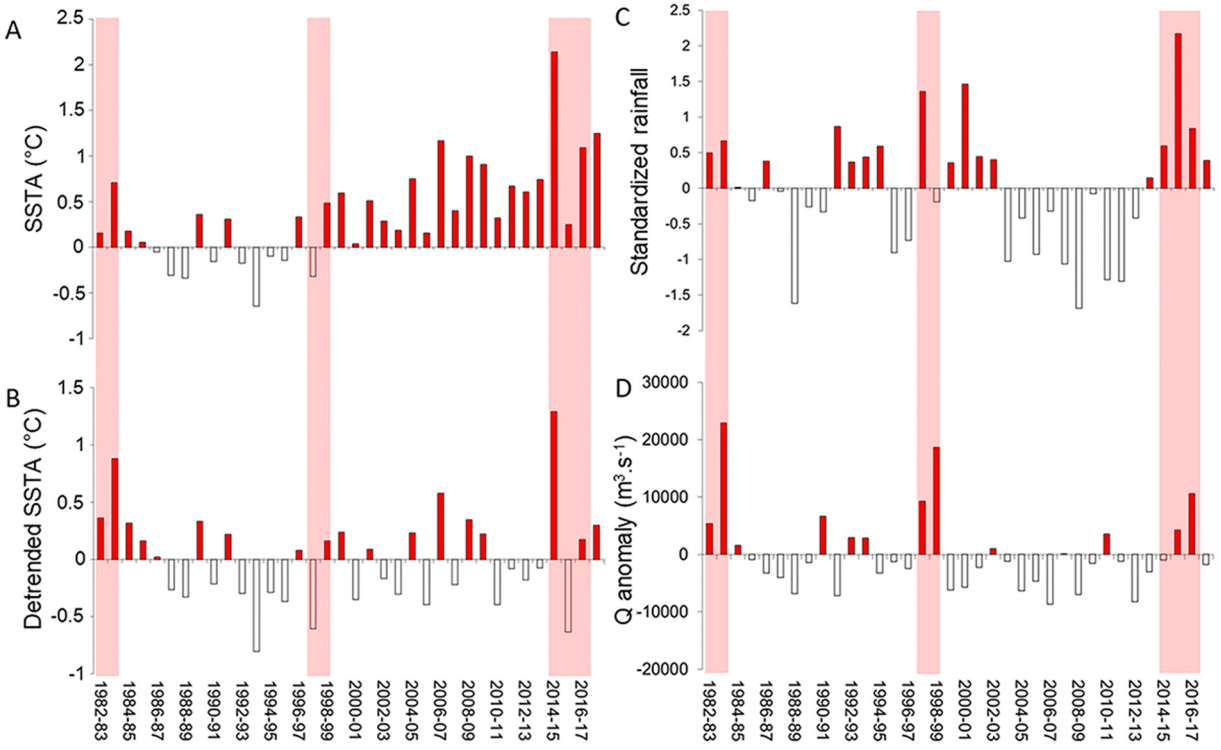

Fig. 2. Long-term (1982–2018) variations during September–April in (A) SSTA and (B) detrended SSTA time series of the SW Atlantic shelf and the adjacent oceanic region and (C) standardized rainfall and (D) Q anomaly in the Río de la Plata basin. Shaded bars highlight the three historical extreme El Niño events.

Table 1
Ecosystem attributes (including flow and organization indicators) of the four Ecopath models for Barra del Chuy beach: baseline (1982), before (2013) and after (spring 2016-autumn 2017, and 2018) the 2015–2016 El Niño event.

Parameter	Baseline 1982[a]	Before 2013	After 2016–17	2018	Unit
Sum of all consumption	823	1479	768	1273	g/m^2/year
Sum of all exports	3000	16,069	56,414	16,236	g/m^2/year
Sum of all respiratory flows	323	731	289	566	g/m^2/year
Sum of all flows into detritus	3193	16,693	56,634	16,618	g/m^2/year
Total system throughput	7339	34,971	114,105	34,695	g/m^2/year
Sum of all production	3645	17,242	57,011	17,242	g/m^2/year
Calculated total net primary production	5129	16,790	56,692	16,790	g/m^2/year
Total primary production/total respiration	10	23	196	30	
Finn's cycling index	1.700	0.710	0.101	0.537	
Net system production	2987	16,059	56,403	16,223	g/m^2/year
Total primary production/total biomass	82	106	167	108	
Total biomass/total throughput	0.005	0.005	0.003	0.004	/year
Total biomass (excluding detritus)	40	158	339	156	g/m^2
Connectance index	0.211	0.189	0.203	0.197	
System omnivory index	0.106	0.066	0.092	0.066	
Total catch of the yellow clam	20.60	3.35	0.45	2.37	t/km^2/year
Ascendency (A%)	47	64	90	66	
Overhead (O%)	53	36	10	34	
Ecopath pedigree index	0.313	0.413	0.418	0.413	
Measure of fit	0.900	1.872	1.951	1.872	

[a] Lercari et al., 2018.

complete understanding to help disentangle factors driving species richness patterns in sandy beaches (Defeo and McLachlan, 2011). The macroinvertebrate dataset was therefore deconstructed considering four different grouping criteria: taxonomic category (molluscs, polychaetes, and crustaceans); beach zone occupied (supralittoral, upper intertidal and low intertidal/subtidal); feeding mode (deposit/detritivores, filter-suspension feeders and predators/scavengers); and development mode (direct and indirect). Finally, the response of individual species to El Niño was also assessed through long-term variations in abundance and biomass.

3. Results

3.1. Climatic trends

A systematic long-term increase in SSTA was recorded (SSTA = 0.033 year$^{-0.24}$, $R^2 = 0.40$; $p < 0.001$), showing a predominance of positive anomalies after 1998 (Fig. 2A). The linear trend indicated a regional warming rate of 0.33 °C per decade, which was particularly noticeable from 2000 onwards (0.50 °C per decade). The 2014–2015 period was particularly warm, recording SSTA >2 °C above climatological values (Fig. 2A) and 1.5 °C for the detrended time series (Fig. 2B). Nevertheless, detrended SSTA evidenced the occurrence of a cold period from September 2015 to April 2016 (Fig. 2B). Standardized rainfall showed the highest values during the three extreme El Niño events that occurred in 1982–1983, 1997–1998, and 2015–2016. In the latter, rainfall in the basin region surpassed more than two standard deviations (Fig. 2C). In this vein, the RdlP displayed high positive Q anomalies during extreme warm ENSO events, with 5000 $m^3 \cdot s^{-1}$ above the historical values for 2015–2016 and 10,000 $m^3 \cdot s^{-1}$ for 2016–2107 (Fig. 2D).

3.2. Ecosystem structure

The consistency of the input data was ensured by PREBAL diagnoses (see Supplementary Materials D and E for PREBAL diagnoses and output data, respectively). Following Lassalle et al. (2014), the overall pedigree index indicated an average to high-quality level of the analysed models (Table 1).

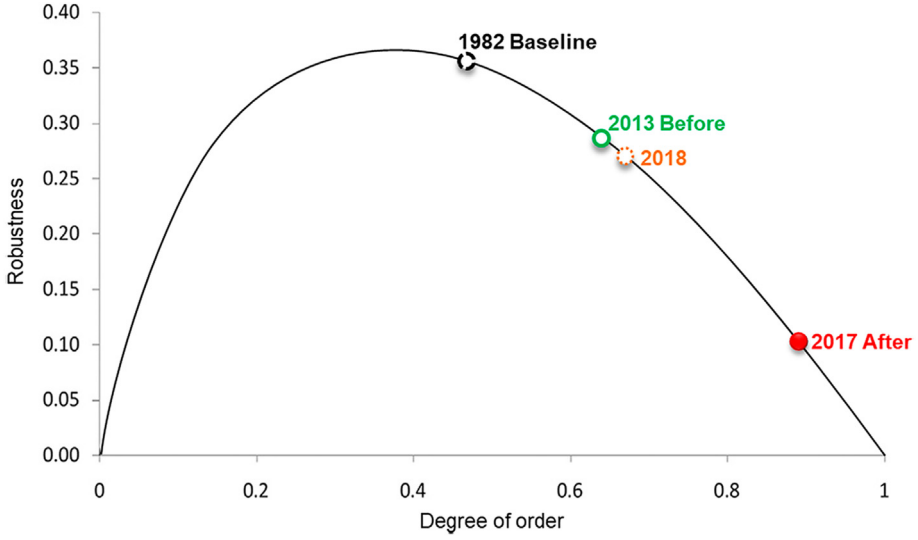

Fig. 3. Long-term variations in Robustness vs. degree of order of the four ecosystem models for Barra del Chuy beach: 1982 (), before (2013) and after (2017 and 2018) El Niño events.

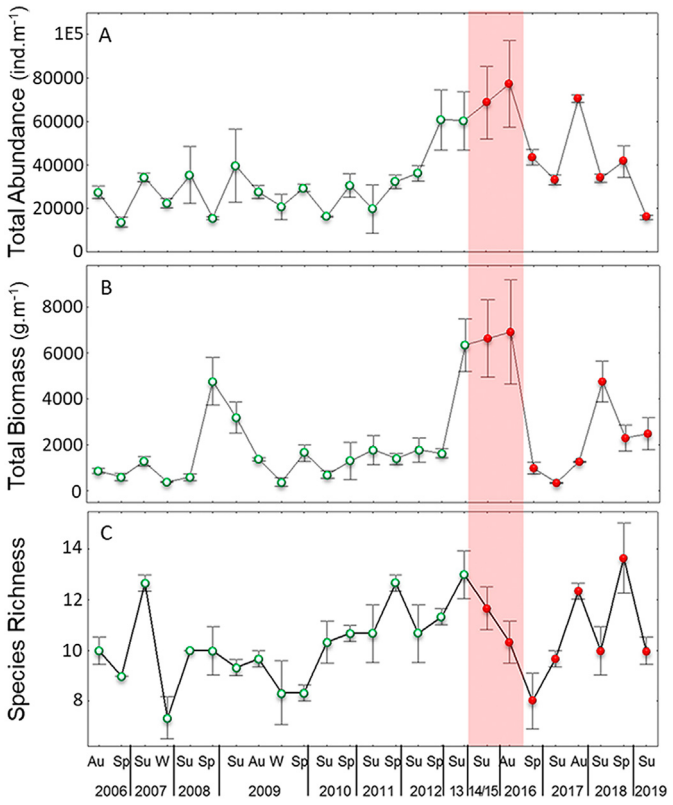

Fig. 4. Long-term fluctuations (2006–2019) in total (mean ± 0.95*SE) macroinvertebrate community abundance (A), biomass (B), and species richness (C) for Barra del Chuy beach, before (○) and during and after (●) the 2015–2016 El Niño event (shaded bar). Au: autumn; W: winter; Sp: spring; Su: summer.

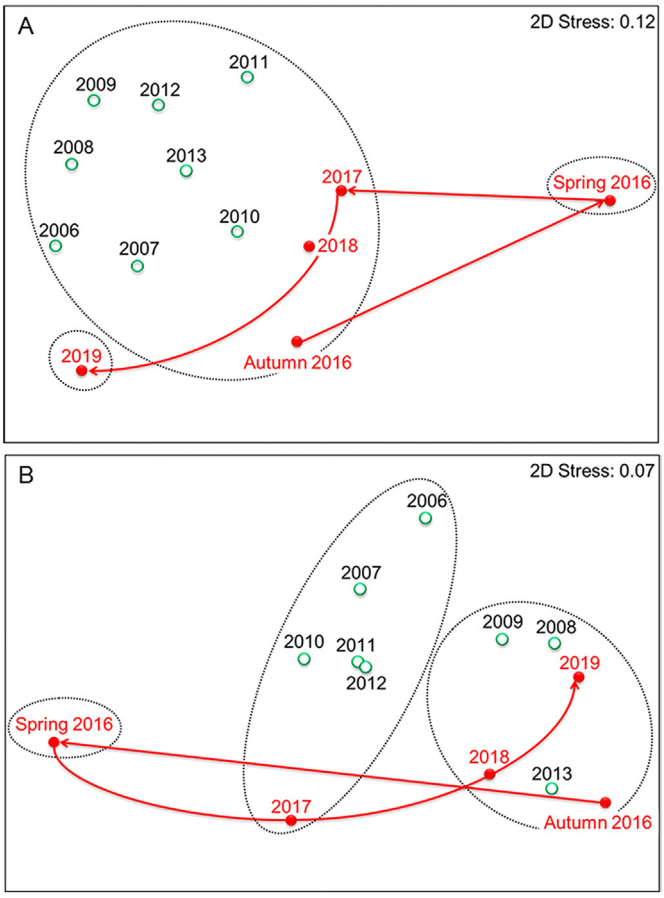

Fig. 5. NMDS ordination according to macroinvertebrate abundance (A) and biomass (B) for Barra del Chuy beach before (○) and during and after (●) the El Niño event. Ellipses indicate the similarity level (60%) from cluster analysis.

Ecosystem indicators showed a rapid and unequivocal effect of the 2015–2016 El Niño event disrupting the internal ecosystem structure and functioning (Table 1 and Fig. 3). The ecosystem size, measured by TST, tripled after the pulse perturbation, returning to pre-event values by 2018. The SOI increased by one-third after El Niño, reaching values similar to the baseline and returning to pre-event values by 2018. After the perturbation, the gap between Ascendency and Overhead was the highest on record. The organization of the flow structure (Ascendency) increased from 64% to 90%, whereas the recovery potential (Overhead) decreased from 36% to 10%, with the consequent decrease in resilience. In 2018, the system still showed an imbalance between attributes but exhibited values similar to the pre-disturbed state. Compared to the baseline, the Robustness analysis revealed a substantial increase in efficiency towards 2013, reaching its highest immediately after El Niño (Fig. 3).

3.3. Community structure

The total abundance and biomass of the macroinvertebrate community (Fig. 4A and B) drastically decreased after El Niño (spring 2016: 72% and 16% of the pre-event values, respectively), a tendency that continued until summer 2017. In 2019, both community attributes reached 26% and 39% of pre-event values, respectively. Species richness reached its lowest value in seven years, immediately after El Niño (Fig. 4C). NMDS ordination based on abundance (Fig. 5A) identified three groups at a similarity level of 65% (stress = 0.12), showing rapid turnover of the community after El Niño but comprising an independent group in 2019. According to biomass (Fig. 5B), NMDS also identified three groups at a similarity level of 60% (stress = 0.07), showing a gradual turnover of the community towards 2019. PERMANOVA showed differences in the community structure before and after El Niño, both for abundance ($t = 2.88$; $p = 0.001$) and biomass ($t = 2.24$; $p = 0.001$).

3.4. Deconstructive approach

The abundance (Fig. 6A–D) and biomass (Fig. 6E–H) of almost all members of the macrofauna markedly decreased after El Niño, except for polychaetes, deposit feeders/detritivores, and upper intertidal species. Taxonomic deconstruction showed that molluscs, which dominated the community abundance and biomass before the pulse perturbation (Fig. 6A and E), sharply decreased after El Niño, exhibiting their lowest abundance since 2006 (spring 2016: less than 3% of the pre-event value). Crustacean abundance and biomass also decreased, representing only 20% and 5% of pre-event values, respectively. By contrast, polychaetes reached their highest abundance since 2006, increasing by a factor of four after El Niño and markedly decreasing afterwards. Deconstruction by feeding group showed that filter feeders dominated the pre-disturbed state and reached their lowest abundance and biomass after El Niño (less than 2% of pre-event values in both cases; Fig. 6B and F). Likewise, predators/scavengers also decreased in abundance (32% of pre-event value), showing no variation in biomass after El Niño. Deposit feeders/detritivores followed a reverse trend in abundance, doubling after El Niño and dominating the community for the following two years. Deconstruction by beach zone occupied showed that low intertidal/subtidal and supralittoral species decreased after El Niño (abundance: 11% and 14%, biomass: 6% and 14% of pre-event values, respectively), while the abundance of upper intertidal species almost doubled after the pulse perturbation, and biomass decreased by half (Fig. 6C and G). Deconstruction by development mode showed that both categories decreased after El Niño (Fig. 6D and H). The

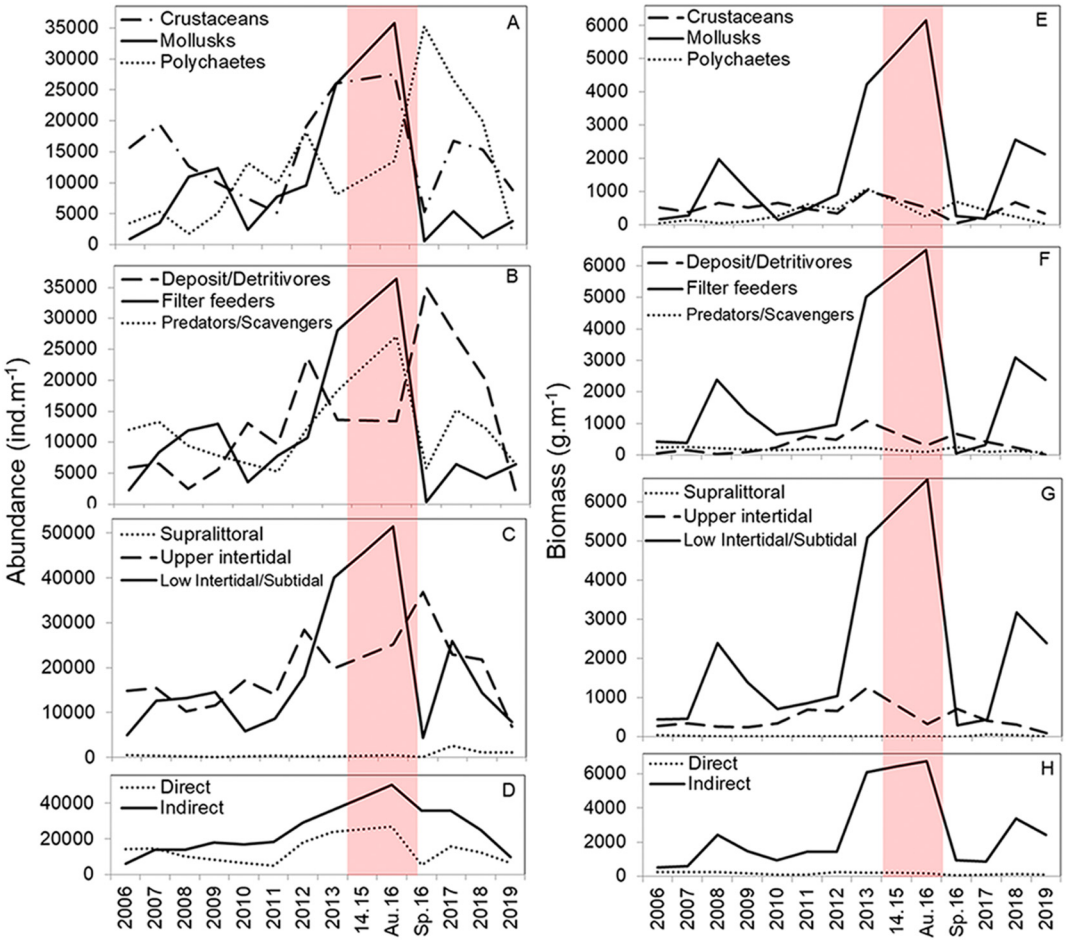

Fig. 6. Long-term fluctuations (2006–2019) in macrofaunal abundance (left panels) and biomass (right panels) deconstructed by taxonomic group (A, E), feeding mode (B, F), beach zone occupied (C, G), and development mode (D, H) for Barra del Chuy beach. Au: autumn; Sp: spring. The shaded bar highlights the 2015–2016 El Niño event.

abundance and biomass of all analysed groups showed negative trends towards 2019.

A substantial change in the relative representation of species abundance and biomass was registered after El Niño (Fig. 7A and B). The yellow clam *M. mactroides* dominated the community before the pulse perturbation (abundance = 34%, biomass = 62%), whereas *Euzonus furcifera* dominated the post-disturbance scenario (spring 2016: abundance = 80%, biomass = 67%) until 2017. After El Niño, *M. mactroides* represented 1% of the total community abundance and 6% of the community biomass (less than 2% of pre-event values in both cases) but showed a marked increase in biomass from 2018 (69% of the community) onwards.

4. Discussion

Long-term data evidenced an abrupt disruption of ecological attributes of the sandy beach system at all levels of ecological organization due to the effects of the extreme 2015–2016 El Niño event. Marked impacts on stability indices (e.g., Robustness), community structure (e.g., abundance, biomass, and species richness), species composition, and dominance stood out. A transitional community state dominated by opportunistic species was set after the pulse perturbation. By 2018, the structural and functional restructuring prompted by El Niño would have increased the vulnerability of the BCB system compared with the pre-disturbed state. This loss of resilience could explain the variability and potentially lagged responses observed by 2019.

The notorious climatic effects of the 2015–2016 El Niño in the study zone were reflected in a marked increase in SSTA and rainfall and in the discharge of the widest estuary of the world (RdlP). These impacts can be attributed in part to the unusually warm conditions in 2014, accompanied by the long-term warming context in the SAO (Ortega et al., 2016; Franco et al., 2020). The detrended time series also denoted high SSTA during the exceptionally warm period 2014–2015. The combination of these stressors derived from a pulse perturbation, together with rising sea levels, increasing onshore winds, and storm surges already documented in the area (Ortega et al., 2013; McLachlan and Defeo, 2018), acted in a synergic way, magnifying the detrimental effects on BCB. This has critical implications for sandy beach ecosystems, which can be considered a narrow land-sea interface extremely vulnerable to a combination of press and pulse climate perturbations (McLachlan and Defeo, 2018). Increased rainfall in the Andreoni Canal basin could also have increased local discharge, causing added impacts (e.g., nutrient enrichment, erosion). However, the effects of the RdlP, which drains the second largest river basin in South America, are drastically higher when compared with local ones (Lercari et al. 2002).

The long-term analysis, which included ecosystem modelling for the last 40 years, unambiguously denoted that BCB is under high pressure derived from the interaction between multiple stressors. Drastic ecosystem effects were quantified in response to the 2015–2016 El Niño, which led to a lower sustainability of the system and an alternative state in 2018. The ecosystem was particularly sensitive to changes in PP. On sandy beaches located in the SAO, El Niño has been described as a strong driver leading significant interannual PP changes (Odebrecht et al., 2014), as rising temperatures and onshore winds could trigger blooms of autochthonous surf diatom populations (Boyce and Worm, 2015). At BCB, *Asterionellopsis guyunusae* could

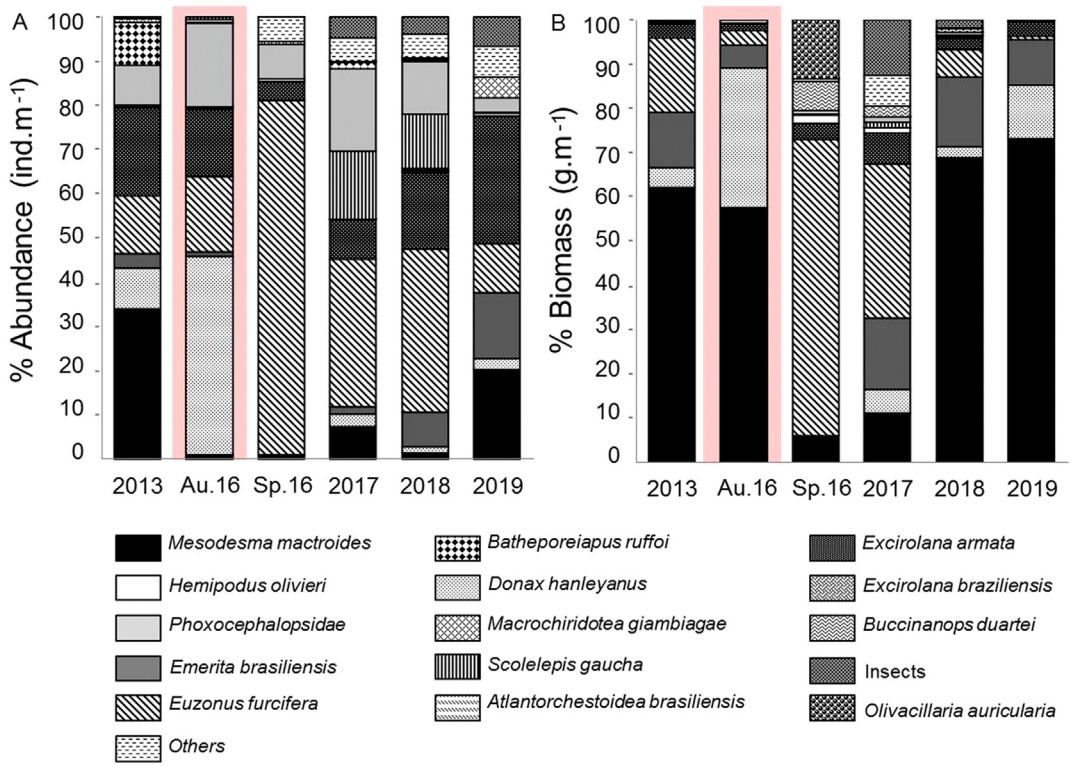

Fig. 7. Fluctuations (2013–2019) in species composition expressed in abundance (A) and biomass (B) for Barra del Chuy beach. Au: autumn; Sp: spring. The shaded bar highlights the 2015–2016 El Niño event.

reach high abundance and elevated PP rates during conditions of high precipitation and freshwater runoff, as observed in similar dissipative beaches on the Brazilian coast (Odebrecht et al., 1995; Reynaldi, 2000; Rörig and Garcia, 2003). This could explain the clear fluctuation in ecosystem flow size measured by TST and in the sum of all production- and PP-related indicators. The increased omnivory (SOI) could indicate an enhancement of system resistance to the impacts driven by El Niño (Christensen and Pauly, 1992), counteracting the magnitude of environmental stress (Odum, 1985; Saint-Béat et al., 2015). However, the lower sustainability of BCB immediately after El Niño, evidenced by the gap between Ascendency and Overhead, could have amplified the vulnerability of the system to cope with stressors (Elliott et al., 2007; Saint-Béat et al., 2015), being unable to recover after two years of the event. The turnover of Ascendency and Overhead to an almost pre-disturbed state by 2018 could have been favoured by the development of the 2017–2018 La Niña event from September 2017 to April 2018 (https://origin.cpc.ncep.noaa.gov/products/analysis_monitoring/ensostuff/ONI_v5.php, last accessed November 2020), favouring cold-water species such as *M. mactroides,* which dominated the community before and during the 2015–2016 El Niño. Furthermore, the deconstructive analysis at the species level revealed that recovery to 2019 was unsuccessful, concurrently with the occurrence of a new El Niño event from September 2018 to July 2019 (https://origin.cpc.ncep.noaa.gov/products/analysis_monitoring/ensostuff/ONI_v5.php, last accessed November 2020). In this sense, the results support that overlapping pressures could compromise (influence or inhibit) the achievement of the pre-disturbed state. Coastal ecosystems are inherently variable, following complex trajectories and exhibiting hysteresis during recovery (Elliott et al., 2007; Borja et al., 2010; Duarte et al., 2015; McLachlan and Defeo, 2018), as seems to be the case for BCB.

The impoverishment of the macrofaunal community, prompted by El Niño, was primarily reflected in abundance, biomass, and species richness in spring 2016. The marked decrease in abundance and biomass continued until summer 2017, leading to a contrasting community state in comparison with the pre-disturbed scenario. Although NMDS suggested a rapid reorganization of the macroinvertebrate community structure, recovery to 2019 was unsuccessful, challenging ecosystem resilience. Sandy-beach macrofauna have shown low adaptive capacity in response to El Niño events (Arntz et al., 2006; McLachlan and Defeo, 2018). Revell et al. (2011) also reported that reductions in invertebrate mean body size and biomass were detected up to two years after the 1997–1998 El Niño in California beaches. The occurrence of CC-related stressors (e.g., sustained increases in storm wave events and onshore winds) acting together could aggravate this scenario. Indeed, SSTA has noticeably increased in the RdlP over the last two decades. This change in the background press, together with the occurrence of extreme pulse events such as El Niño, may influence community responses, as observed in other systems (Harris et al., 2018, 2020).

Faunal groups were affected to a dissimilar extent. Molluscs, filter feeders, and low intertidal/subtidal groups showed a sharply negative response to El Niño-driven changes. A transitional community dominated by the opportunistic polychaete *E. furcifera* was set after pulse perturbation due to an enhancement in food availability, as freshwater runoff produced short-term deposition of organic matter from terrestrial sources (Lopes Costa et al., 2020). Freshwater runoff could have also modified sediment compaction and moisture, favouring the microorganism associations from which deposits/detritivores feed (Otegui et al., 2012). The same pattern was found on South Pacific beaches, where El Niño prompted the establishment of a macrofaunal community dominated by small opportunistic polychaetes (Arntz et al., 1987).

Changes in community biomass were strongly driven by shifts in the clam *M. mactroides*. The dramatic decrease in its abundance during El Niño events has been associated with the combined effects of the increasing trend in SST since the late 1990s (Ortega et al., 2012) and the characteristic positive SSTA during these events (Barreiro, 2010), which negatively affect this mollusc with cold-water affinities (Ortega et al., 2016). By contrast, this scenario favoured warm-water species such as the wedge clam *Donax hanleyanus* and the mole crab *E. brasiliensis*, which are subordinate competitors for space and food in this suspension-feeding guild (Ortega et al., 2012; Defeo et al., 2013;

Celentano and Defeo, 2016). A high abundance of *M. mactroides* tends to occur during La Niña years, characterized by a cyclonic configuration of wind stress anomalies in the SAO, with cold and salty waters and onshore wind stress anomalies on the Uruguayan Atlantic coast (Manta et al., 2018). In this sense, detrended SSTA evidenced the occurrence of a cold period from September 2015 to April 2016, explaining the high macroinvertebrate community abundance and biomass, despite the development of El Niño. As previously registered in BCB, a drastic decrease in the abundance of dominant species such as *M. mactroides* would have a significant negative impact on the marine food web, modifying ecosystem functioning and therefore the provision of ecosystem services (Lercari et al., 2018; Jorge-Romero et al., 2019). A progressive loss of habitat suitability, together with spawning and recruitment failures at suboptimum conditions, could trigger overall long-term population declines (McLachlan and Defeo, 2018), affecting the structure of the community and constraining the functioning of the sandy beach ecosystem (Jorge-Romero et al., 2019). These findings support the perception that disturbances can alter ecological interactions and therefore contribute to the simplification and destabilization of coastal ecosystems (McCauley et al., 2012).

5. Conclusions and prospects

This study adds new insights into El Niño-induced changes in sandy beach ecosystems, highlighting how extreme climatic events can result in strong responses at different levels of ecological organization. Profound changes in relative species abundance and biomass shifted the structure of the macroinvertebrate community. In addition, increased PP and the concomitant boost in TST led the system to a state of a higher degree of order and lower Robustness. The negative trends observed in 2019 suggest a higher vulnerability of the BCB system to cope with climate-driven changes, supporting the occurrence of prolonged recovery periods and hysteresis. Thus, it cannot be assumed that sandy beach ecosystems will immediately recover when perturbations disappear or shrink. The results become even more relevant in the context of one of the largest and most energetic warming hotspots worldwide. However, the formal detection and attribution of biological responses to a compounding impact of press (CC) and pulse (e.g., El Niño, La Niña) perturbations is highly challenging, particularly in sandy beach ecosystems, whose macrofauna have wide natural fluctuations in abundance and are extremely sensitive to environmental variations. A critical step will be to quantify the relative influence of these drivers, operating simultaneously at different spatial and temporal scales, as well as the mechanisms operating behind the observed changes. This is of utmost importance in sandy beaches, which have been recognized as ecosystems at risk that are being increasingly threatened by long-lasting climate-driven stressors (McLachlan and Defeo, 2018).

Funding

This work was supported by Comisión Sectorial de Investigación Científica (CSIC-Grupos ID 32, C801-348 PIP), and the Inter-American Institute for Global Change Research (grant CRN 3070, Small-scale Fisheries and Marine Ecosystem Services: Adaptation and Transformation to Secure Human Wellbeing, SGP-HW 017 project).

CRediT authorship contribution statement

Gabriela Jorge-Romero: Conceptualization, Methodology, Formal analysis, Data curation, Writing – original draft, Visualization, Supervision. **Eleonora Celentano:** Conceptualization, Methodology, Formal analysis, Writing – review & editing, Visualization. **Diego Lercari:** Conceptualization, Methodology, Formal analysis, Resources, Writing – review & editing, Funding acquisition. **Leonardo Ortega:** Conceptualization, Methodology, Formal analysis, Writing – review & editing, Visualization. **Juan A. Licandro:** Writing – review & editing. **Omar Defeo:** Conceptualization, Methodology, Resources, Writing – review & editing, Project administration, Funding acquisition.

Declaration of competing interest

The authors declare that they have no known competing financial interests or personal relationships that could have appeared to influence the work reported in this paper.

Acknowledgements

This work is part of G. Jorge-Romero PhD thesis. We thank the Benthic Ecology Group from UNDECIMAR for field and laboratory assistance. A referee provided very useful suggestions that improved the manuscript.

Appendix A. Supplementary data

Supplementary data to this article can be found online at https://doi.org/10.1016/j.scitotenv.2021.145689.

References

Anderson, M.J., Gorley, R.N., Clarke, K.R., 2015. PERMANOVA+ for PRIMER: Guide to Software and Statistical Methods (PRIMER-E).
Arntz, W.E., Brey, T., Tarazona, J., Robles, A., 1987. Changes in the structure of a shallow sandy-beach community in Peru during an El Niño event. S. Afr. J. Mar. Sci. 5, 645–658.
Arntz, W.E., Gallardo, V.A., Gutiérrez, D., Isla, E., Levin, L.A., Mendo, J., Neira, C., Rowe, G.T., Tarazona, J., Wolff, M., 2006. El Niño and similar perturbation effects on the benthos of the Humboldt, California, and Benguela current upwelling ecosystems. Adv. Geosci. 6, 243–265.
Barnard, P.L., Hoover, D., Hubbard, D.M., Snyder, A., Ludka, B.C., Allan, J., Kaminsky, G.M., Ruggiero, P., Gallien, T.W., Gabel, L., McCandless, D., 2017. Extreme oceanographic forcing and coastal response due to the 2015–2016 El Niño. Nat. Commun. 8, 1–8.
Barreiro, M., 2010. Influence of ENSO and the South Atlantic Ocean on climate predictability over southeastern South America. Clim. Dyn. 35, 1493–1508.
Bertrand, A., Lengaigne, M., Takahashi, K., Avadí, A., Poulain, F., Harrod, C., 2020. El Niño Southern Oscillation (ENSO) effects on fisheries and aquaculture. FAO Fisheries and Aquaculture Technical Paper No. 660. FAO, Rome.
Bindoff, N.L., Cheung, W.W., Kairo, J.G., Arstegui, J., Guinder, V.A., Hallberg, R., Hilmi, N., Jiao, N., Karim, M.S., Levin, L., O'Donoghue, S., Purca Cuicapusa, S.R., Rinkevich, B., Suga, T., Tagliabue, A., Williamson, P., 2019. Changing ocean, marine ecosystems, and dependent communities. IPCC Special Report on the Ocean and Cryosphere in a Changing Climate.
Bodnariuk, N., Simionato, C.G., Osman, M., Saraceno, M., 2021. The Río de la Plata plume dynamics over the southwestern Atlantic continental shelf and its link with the large scale atmospheric variability on interannual timescales. Cont. Shelf Res. 212, 104296.
Borja, Á., Dauer, D.M., Elliott, M., Simenstad, C.A., 2010. Medium-and long-term recovery of estuarine and coastal ecosystems: patterns, rates and restoration effectiveness. Estuar. Coasts 33, 1249–1260.
Boyce, D.G., Worm, B., 2015. Patterns and ecological implications of historical marine phytoplankton change. Mar. Ecol. Prog. Ser. 534, 251–272.
Brazeiro, A., Defeo, O., 1996. Macroinfauna zonation in microtidal sandy beaches: is it possible to identify patterns in such variable environments? Estuar. Coast. Shelf Sci. 42, 523–536.
Brey, T., 2012. A multi-parameter artificial neural network model to estimate macrobenthic invertebrate productivity and production. Limnol. Oceanogr. Methods 10, 581–589.
Cai, W., Borlace, S., Lengaigne, M., Van Rensch, P., Collins, M., Vecchi, G., Timmermann, A., Santoso, A., McPhaden, M.J., Wu, L., England, M.H., Wang, G., Guilyardi, E., Jin, F., 2014. Increasing frequency of extreme El Niño events due to greenhouse warming. Nat. Clim. Chang. 4, 111–116.
Cai, W., McPhaden, M.J., Grimm, A.M., Rodrigues, R.R., Taschetto, A.S., Garreaud, R.D., Dewitte, B., Poveda, G., Ham, Y.G., Santoso, A., Ng, B., Anderson, W., Wang, G., Geng, T., Jo, H., Marengo, J., Alves, L., Osman, M., Li, S., Wu, L., Karamperidou, C., Takahashi, K., Vera, C., 2020. Climate impacts of the El Niño–southern oscillation on South America. Nat. Rev. Earth Environ. 1, 215–231.
Cavalieri, D.J., Parkinson, C.L., Gloersen, P., Zwally, H.J., 1997. Sea Ice Concentrations from Nimbus-7 SMMR and DMSP SSM/I Passive Microwave Data, June to September 2001. Boulder, CO, USA updated 2005.
Cavanaugh, K.C., Reed, D.C., Bell, T.W., Castorani, M.C., Beas-Luna, R., 2019. Spatial variability in the resistance and resilience of giant kelp in southern and Baja California to a multiyear heatwave. Front. Mar. Sci. 6, 413.
Cazes-Boezio, G., Robertson, A.W., Mechoso, C.R., 2003. Seasonal dependence of ENSO teleconnections over South America and relationships with precipitation in Uruguay. J. Clim. 16, 1159–1176.
Celentano, E., Defeo, O., 2016. Effects of climate on the mole crab *Emerita brasiliensis* on a dissipative beach in Uruguay. Mar. Ecol. Prog. Ser. 552, 211–222.
Christensen, V., Pauly, D., 1992. ECOPATH II - a software for balancing steady-state ecosystem models and calculating network characteristics. Ecol. Model. 61, 169–185.
Christensen, V., Pauly, D., 1998. Changes in models of aquatic ecosystems approaching carrying capacity. Ecol. Appl. 8, 104–109.

Christensen, V., Walters, C.J., 2004. Ecopath with Ecosim: methods, capabilities and limitations. Ecol. Model. 172, 109–139.
Christensen, V., Walters, C.J., Pauly, D., 2005. Ecopath with Ecosim: A user's Guide. Fisheries Centre, University of British Columbia, Vancouver 154 pp.
Christensen, V., Walters, C.J., Pauly, D., Forrest, R., 2008. Ecopath with Ecosim version 6 user guide. Lenfest Ocean Futures Project 235 pp.
Cremella, B., Huot, Y., Bonilla, S., 2018. Interpretation of total phytoplankton and cyanobacteria fluorescence from cross-calibrated fluorometers, including sensitivity to turbidity and colored dissolved organic matter. Limnol. Oceanogr. Methods 16, 881–894.
Defeo, O., McLachlan, A., 2011. Coupling between macrofauna community structure and beach type: a deconstructive meta-analysis. Mar. Ecol. Prog. Ser. 433, 29–41.
Defeo, O., McLachlan, A., Schoeman, D.S., Schlacher, T.A., Dugan, J., Jones, A., Lastra, M., Scapini, F., 2009. Threats to sandy beach ecosystems: a review. Estuar. Coast. Shelf Sci. 81, 1–2.
Defeo, O., Castrejón, M., Ortega, L., Kuhn, A.M., Gutiérrez, N.L., Castilla, J.C., 2013. Impacts of climate variability on Latin American small-scale fisheries. Ecol. Soc. 18 (4), 30.
Duarte, C.M., Borja, A., Carstensen, J., Elliott, M., Krause-Jensen, D., Marbà, N., 2015. Paradigms in the recovery of estuarine and coastal ecosystems. Estuar. Coasts 38 (4), 1202–1212.
Elliott, M., Burdon, D., Hemingway, K.L., Apitz, S.E., 2007. Estuarine, coastal and marine ecosystem restoration: confusing management and science–a revision of concepts. Estuar. Coast. Shelf Sci. 74, 349–366.
Fanini, L., Defeo, O., Elliott, M., 2020. Advances in sandy beach research-local and global perspectives. Estuar. Coast. Shelf Sci. 234, 106646.
Fath, B.D., 2015. Quantifying economic and ecological sustainability. Ocean Coast. Manag. 108, 13–19.
Franco, B.C., Defeo, O., Piola, A.R., Barreiro, M., Yang, H., Ortega, L., Gianelli, I., Castello, J.P., Vera, C., Buratti, C., Pájaro, M., 2020. Climate change impacts on the atmospheric circulation, ocean, and fisheries in the southwest South Atlantic Ocean: a review. Clim. Chang. 162, 2359–2377.
Gianelli, I., Ortega, L., Marín, Y., Piola, A.R., Defeo, O., 2019a. Evidence of ocean warming in Uruguay's fisheries landings: the mean temperature of the catch approach. Mar. Ecol. Prog. Ser. 625, 115–125.
Gianelli, I., Ortega, L., Defeo, O., 2019b. Modeling short-term fishing dynamics in a small-scale intertidal shellfishery. Fish. Res. 209, 242–250.
Grumbine, R.W., 1996. Automated Passive Microwave Sea Ice Concentration Analysis at NCEP. NOAA Tech. Note 120. 13 pp. Available from. NCEP/NWS/NOAA, 5200 Auth Road, Camp Springs, MD 20746, USA.
Harris, R.M., Beaumont, L.J., Vance, T.R., Tozer, C.R., Remenyi, T.A., Perkins-Kirkpatrick, S.E., Mitchell, P.J., Nicotra, A.B., McGregor, S., Andrew, N.R., Letnic, M., 2018. Biological responses to the press and pulse of climate trends and extreme events. Nat. Clim. Chang. 8, 579–587.
Harris, R.M., Loeffler, F., Rumm, A., Fischer, C., Horchler, P., Scholz, M., Foeckler, F., Henle, K., 2020. Biological responses to extreme weather events are detectable but difficult to formally attribute to anthropogenic climate change. Sci. Rep. 10, 14067.
Herring, S.C., Christidis, N., Hoell, A., Kossin, J.P., Schreck III, C.J., Stott, P.A., 2018. Explaining extreme events of 2016 from a climate perspective. Bull. Am. Meteorol. Soc. 99, S1–S157.
Heymans, J.J., Coll, M., Link, J.S., Mackinson, S., Steenbeek, J., Walters, C., Christensen, V., 2016. Best practice in Ecopath with Ecosim food-web models for ecosystem-based management. Ecol. Model. 331, 173–184.
Hobday, A.J., Pecl, G.T., 2014. Identification of global marine hotspots: sentinels for change and vanguards for adaptation action. Rev. Fish Biol. Fish. 24, 415–425.
Janowiak, J.E., Gruber, A., Kondragunta, C.R., Livezey, R.E., Huffman, G.J., 1999. A comparison of the NCEP–NCAR reanalysis precipitation and the GPCP rain gauge–satellite combined dataset with observational error considerations. J. Clim. 11, 2960–2979.
Jorge-Romero, G., Lercari, D., Ortega, L., Defeo, O., 2019. Long-term ecological footprints of a man-made freshwater discharge onto a sandy beach ecosystem. Ecol. Indic. 96, 412–420.
Lassalle, G., Bourdaud, P., Saint-Béat, B., Rochette, S., Niquil, N., 2014. A toolbox to evaluate data reliability for whole-ecosystem models: application on the Bay of Biscay continental shelf food-web model. Ecol. Model. 285, 13–21.
Lercari, D., Defeo, O., 2006. Large-scale diversity and abundance trends in sandy beach macrofauna along full gradients of salinity and morphodynamics. Estuar. Coast. Shelf Sci. 68, 27–35.
Lercari, D., Defeo, O., 2015. Large-scale dynamics of sandy beach ecosystems in transitional waters of the southwestern Atlantic Ocean: species turnover, stability and spatial synchrony. Estuar. Coast. Shelf Sci. 154, 184–193.
Lercari, D., Defeo, O., Celentano, E., 2002. Consequences of a freshwater canal discharge on the benthic community and its habitat on an exposed sandy beach. Mar. Pollut. Bull 44, 1392–1399.
Lercari, D., Bergamino, L., Defeo, O., 2010. Trophic models in sandy beaches with contrasting morphodynamics: comparing ecosystem structure and biomass flow. Ecol. Model. 221, 2751–2759.
Lercari, D., Defeo, O., Ortega, L., Orlando, L., Gianelli, I., Celentano, E., 2018. Long-term structural and functional changes driven by climate variability and fishery regimes in a sandy beach ecosystem. Ecol. Model. 368, 41–51.
Link, J.S., 2010. Adding rigor to ecological network models by evaluating a set of prebalance diagnostics: a plea for PREBAL. Ecol. Model. 21, 1580–1591.
Lopes Costa, L., Zalmon, I.R., Fanini, L., Defeo, O., 2020. Macroinvertebrates as indicators of human disturbances on sandy beaches: a global review. Ecol. Indic. 118, 106764.
Manta, G., de Mello, S., Trinchin, R., Badagian, J., Barreiro, M., 2018. The 2017 record marine heatwave in the southwestern Atlantic shelf. Geophys. Res. Lett. 45, 12449–12456.
Martínez, A., Méndez, S., Fabre, A., Ortega, L., 2017. Intensificación de floraciones de dinoflagelados marinos en Uruguay. INNOTEC 13, 19–25.
May, D.A., Parmeter, M.M., Olszewski, D.S., McKenzie, B.D., 1998. Operational processing of satellite sea surface temperature retrievals at the naval oceanographic office. Bull. Am. Meteorol. Soc. 79, 397–408.
McCauley, D.J., DeSalles, P.A., Young, H.S., Dunbar, R.B., Dirzo, R., Mills, M.M., Micheli, F., 2012. From wing to wing: the persistence of long ecological interaction chains in less-disturbed ecosystems. Sci. Rep. 2, 409.
McLachlan, A., Defeo, O., 2018. The Ecology of Sandy Shores. third ed. Academic Press, United Kingdom.
McLachlan, A., Defeo, O., Jaramillo, E., Short, A.D., 2013. Sandy beach conservation and recreation: guidelines for optimising management strategies for multi-purpose use. Ocean Coast. Manag. 71, 256–268.
Mumby, P.J., Chollett, I., Bozec, Y.M., Wolff, N.H., 2014. Ecological resilience, robustness and vulnerability: how do these concepts benefit ecosystem management? Curr. Opin. Environ. Sustain. 7, 22–27.
Odebrecht, C., Segatto, A.Z., Freitas, C.A., 1995. Surf-zone chlorophyll a variability at Cassino Beach, southern Brazil. Estuar. Coast. Shelf Sci. 41, 81–90.
Odebrecht, C., Du Preez, D.R., Abreu, P.C., Campbell, E.E., 2014. Surf zone diatoms: a review of the drivers, patterns and role in sandy beaches food chains. Estuar. Coast. Shelf Sci. 150, 24–35.
Odum, E.P., 1985. Trends expected in stressed ecosystems. Bioscience 35, 419–422.
Orlando, L., Ortega, L., Defeo, O., 2019. Multi-decadal variability in sandy beach area and the role of climate forcing. Estuar. Coast. Shelf Sci. 218, 197–203.
Ortega, L., Martínez, A., 2007. Multiannual and seasonal variability of water masses and fronts over the Uruguayan shelf. J. Coast. Res. 23, 618–629.
Ortega, L., Castilla, J.C., Espino, M., Yamashiro, C., Defeo, O., 2012. Effects of fishing, market price, and climate on two south American clam species. Mar. Ecol. Prog. Ser. 469, 71–85.
Ortega, L., Celentano, E., Finkl, C., Defeo, O., 2013. Effects of climate variability on the morphodynamics of Uruguayan sandy beaches. J. Coast. Res. 29, 747–755.
Ortega, L., Celentano, E., Delgado, E., Defeo, O., 2016. Climate change influences on abundance, individual size and body abnormalities in a sandy beach clam. Mar. Ecol. Prog. Ser. 545, 203–213.
Otegui, M.B., Blankensteyn, A., Pagliosa, P.R., 2012. Population structure, growth and production of *Thoracophelia furcifera* (Polychaeta: Opheliidae) on a sandy beach in southern Brazil. Helgol. Mar. Res. 66, 479–488.
Pauly, D., Christensen, V., Walters, C., 2000. Ecopath, Ecosim, and Ecospace as tools for evaluating ecosystem impact of fisheries. ICES J. Mar. Sci. 57, 697–706.
Piola, Alberto R., Matano, R.P., Palma, E.D., Möller, O.O., Campos, E.J.D., 2005. The influence of the Plata River discharge on the western South Atlantic shelf. Geophys. Res. Lett. 32, L01603.
Pisciottano, G., Díaz, A., Cazess, G., Mechoso, C.R., 1994. El Niño-southern oscillation impact on rainfall in Uruguay. J. Clim. 7, 1286–1302.
Polovina, J.J., 1984. Model of a coral reef ecosystem. Part I. The ECOPATH model and its application to French Frigate Shoals. Coral Reefs 3, 1–11.
Revell, D.L., Dugan, J.E., Hubbard, D.M., 2011. Physical and ecological responses of sandy beaches to the 1997–98 El Niño. J. Coast. Res. 27, 718–730.
Reynaldi, S., 2000. Efeito da diatomácea de zona de arrebentação *Asterionellopsis glacialis* (Castracane) Round, sobre o crescimento bacteriano na praia do Cassino RS, Brasil. Doctoral dissertation. Federal University of Rio Grande, Brazil.
Reynolds, R.W., Smith, T.M., Liu, C., Chelton, D.B., Casey, K.S., Schlax, M.G., 2007. Daily high-resolution-blended analyses for sea surface temperature. J. Clim. 20, 5473–5496.
Riascos, J.M., Carstensen, D., Laudien, J., Arntz, W.E., Oliva, M.E., Güntner, A., Heilmayer, O., 2009. Thriving and declining: climate variability shaping life-history and population persistence of *Mesodesma donacium* in the Humboldt Upwelling System. Mar. Ecol. Prog. Ser. 385, 151–163.
Robertson, A.W., Mechoso, C.R., 1998. Interannual and decadal cycles in river flows of southeastern South America. J. Clim. 11, 2570–2581.
Robertson, A.W., Mechoso, C.R., 2003. Circulation regimes and low-frequency oscillations in the South Pacific sector. Mon. Weather Rev. 131, 1566–1576.
Rörig, L.R., Garcia, V.M., 2003. Accumulations of the surf-zone diatom *Asterionellopsis glacialis* (Castracane) round in Cassino Beach, southern Brazil, and its relationship with environmental factors. J. Coast. Res. 35, 167–177.
Saint-Béat, B., Baird, D., Asmus, H., Asmus, R., Bacher, C., Pacella, S.R., Johnson, G.A., David, V., Vézina, A.F., Niquil, N., 2015. Trophic networks: how do theories link ecosystem structure and functioning to stability properties? A review. Ecol. Indic. 52, 458–471.
Santoso, A., Mcphaden, M.J., Cai, W., 2017. The defining characteristics of ENSO extremes and the strong 2015/2016 El Niño. Rev. Geophys. 55, 1079–1129.
Schoeman, D.S., Schlacher, T.A., Defeo, O., 2014. Climate-change impacts on sandy-beach biota: crossing a line in the sand. Glob. Chang. Biol. 20, 2383–2392.
Smith, M.D., 2011. An ecological perspective on extreme climatic events: a synthetic definition and framework to guide future research. J. Ecol. 99, 656–663.
Ulanowicz, R.E., 1986. A phenomenological perspective of ecological development. Aquatic Toxicology and Environmental Fate. Ninth Volume. ASTM International.
Ulanowicz, R.E., 2004. Quantitative methods for ecological network analysis. Comput. Biol. Chem. 28, 321–339.
Ulanowicz, R.E., 2014. Reckoning the nonexistent: putting the science right. Ecol. Model. 293, 22–30.
Wang, B., Luo, X., Yang, Y.M., Sun, W., Cane, M.A., Cai, W., Yeh, S.W., Liu, J., 2019. Historical change of El Niño properties sheds light on future changes of extreme El Niño. Proc. Natl. Acad. Sci. 116, 22512–22517.
Wolter, K., 1987. The southern oscillation in surface circulation and climate over the tropical Atlantic, eastern Pacific, and Indian oceans as captured by cluster analysis. J. Clim. Appl. Meteorol. 26, 540–558.